Diffraction and Low-x

Semihard Interactions at TeV energies

Thomas Ventura Iser*
Collaborator: Emerson Luna**

Universidade Federal do Rio Grande do Sul
thomas.iser@ufrgs.br*
luna@if.ufrgs.br**

UFRGS 85 ANOS 1934 - 2019

60 ANOS Instituto de Física

CNPq

- Motivation
- Objective
- QCD Inspired Model
- Analysis
- Results
- Conclusions and Perspectives

Motivation

- To study the behavior of the forward observables, **total cross section** and the ratio of the real to imaginary parts of the scattering amplitude, **ρ**, at LHC-energies, utilizing a QCD-based formalism.

- To explore the tension between experimental results of **ALFA/ATLAS** and **TOTEM** collaborations as off the **difference** between the sets and investigate the possibility of utilizing them together in an analysis.

Objective

❖ To describe the experimental data for **total cross section** and the ratio of the real to imaginary parts of the forward scattering amplitude, **ρ(s)**, in **pp** and **$p\bar{p}$** channels.

- ➢ **Eikonal representation.**
- ➢ **QCD inspired model.**
- ➢ **Integral dispersion relations**.
- ➢ Utilizing **ALFA/ATLAS** and **TOTEM** data sets.
- ➢ Working in **Next-to-Leading Order Scheme**.
- ➢ Updated results utilizing PDF set: **CT18**

The Model

QCD-Inspired Models

Currently, the observed **increase in total cross sections** is well explained by the **QCD-inspired formalism**.

- Here, the **energy dependence** of **total cross sections** is derived from **QCD** utilizing an **eikonal formulation**, which is compatible with **unitarity** and **analicity** constraints.
- The **forward observables** are obtained from the **QCD parton model**.
- Utilizing elementary **QCD parton-parton** processes, updated set of **PDF** and a **cutoff**, physically-motivated, to restrict ourselves to **semihard** parton-level processes only.

Semihard Processes

These come from **hard scatterings** of **partons** carrying **very small fractions of the momenta** of their **parent hadrons**.

- Which leads to the appearance of **jets** with **transverse energy** much smaller than **√s**.
- Here, the scattering of hadrons is an **incoherent summation** over **all possible constituent scattering**.
- Resulting in the **increase** of the **total cross sections** being directly associated with **parton-parton semihard scatterings**.
- The **gluon** plays a role in the **energy dependence** of **cross sections**, since it gives the **dominant contribution** for **$x \ll 1$**.

Profile function and Scattering Amplitude

$$A(s,t) = i \int b \, \mathrm{d}b \, J_0(b\sqrt{-t}) \Gamma(b,s)$$

Fourier-Bessel ↕ Transform

$$\Gamma(b,s) = -i \int_0^\infty q \, \mathrm{d}q \, A(s,t) J_0(bq)$$

Eikonal Representation - Observables

$$\sigma_{el}(s) = 2\pi \int_0^\infty b\,\mathrm{d}b\,|\Gamma(b,s)|^2$$
$$= 2\pi \int_0^\infty b\,\mathrm{d}b\,|1 - e^{-\chi_I(b,s)+i\chi_R(b,s)}|^2$$

$$\sigma_{inel}(s) = 2\pi \int_0^\infty b\,\mathrm{d}b\,G_{inel}(b,s)$$
$$= 2\pi \int_0^\infty b\,\mathrm{d}b\,\left[1 - e^{-2\chi_I(b,s)}\right]$$

$$2\mathrm{Re}\{\Gamma(b,s)\} = |\Gamma(b,s)|^2 + G_{inel}(b,s)$$

$$\sigma_{tot}(s) = 4\pi \int_0^\infty b\,\mathrm{d}b\,\mathrm{Re}\{\Gamma(b,s)\}$$
$$= 4\pi \int_0^\infty b\,\mathrm{d}b\,\left[1 - e^{-\chi_I(b,s)} \cos\chi_R(b,s)\right]$$

$$\rho(s) = \frac{\mathrm{Re}\{i\int b\,\mathrm{d}b[1 - e^{i\chi(b,s)}]\}}{\mathrm{Im}\{i\int b\,\mathrm{d}b[1 - e^{i\chi(b,s)}]\}}$$

$$\Gamma(b,s) \equiv 1 - e^{i\chi(b,s)}$$

The Eikonal Function

$$\chi_{pp}^{\bar{p}p}(s,b) = \chi^{+}(s,b) \pm \chi^{-}(s,b)$$

$$\chi(s,b) = \mathrm{Re}\chi(s,b) + \mathrm{Im}\chi(s,b) \equiv \chi_R(s,b) + i\chi_I(s,b)$$

$$\chi(s,b) = \chi_{soft}(s,b) + \chi_{SH}(s,b)$$

Semihard Contribution

$$\mathrm{Re}\left\{\chi_{SH}(s,b)\right\} = \frac{1}{2} W_{SH}(b)\sigma_{QCD}(s)$$

$$W_{SH}(b) = \int \mathrm{d}^2 b'\, \rho_A\left(|\mathbf{b} - \mathbf{b}'|\right)\rho_B(b')$$

C. A. S. Bahia, M. Broilo, and E. G. S. Luna, Phys. Rev. D 92, 074039 (2015).

Dispersion Relations

$$\mathrm{Im}\left\{\chi^{+}(s,b)\right\} = -\frac{2s}{\pi}\mathcal{P}\int_{0}^{\infty} ds' \frac{\mathrm{Re}\left\{\chi^{+}(s',b)\right\}}{s'^{2}-s^{2}}$$

$$\mathrm{Im}\left\{\chi^{-}(s,b)\right\} = -\frac{2s^{2}}{\pi}\mathcal{P}\int_{0}^{\infty} ds' \frac{\mathrm{Re}\left\{\chi^{-}(s',b)\right\}}{s'(s'^{2}-s^{2})}$$

Soft Contribution

Even Counterpart

$$\chi^{+}_{soft}(s,b) = \frac{1}{2} W^{+}_{soft}(b;\mu^{+}_{soft}) \left[A' + iB' + C' \frac{e^{i\pi\gamma/2}}{(s/s_0)^{\gamma}} \right]$$

Odd Counterpart

$$\chi^{-}_{soft}(s,b) = \frac{1}{2} W^{-}_{soft}(b;\mu^{-}_{soft})\, D' \frac{e^{-i\pi/4}}{\sqrt{s/s_0}}$$

Overlap density and Form factor

$$W(b) = \int \mathrm{d}^2 b' \, \rho_A(|\mathbf{b} - \mathbf{b}'|)\rho(b')$$

$$= \frac{1}{2\pi} \int_0^\infty \mathrm{d}k_\perp \, k_\perp J_0(k_\perp b) G_A(k_\perp) G_B(k_\perp)$$

$$G_A(k_\perp) = G_B(k_\perp) \equiv G_{dip}(k_\perp; \mu) = \left(\frac{\mu^2}{k_\perp^2 + \mu^2} \right)^2$$

$$W_{SH}(b; \nu_{SH}) = \frac{\nu_{SH}^2}{96\pi} (\nu_{SH} b)^3 K_3(\nu_{SH} b)$$

$$\rho(b) = \frac{1}{(2\pi)^2} \int \mathrm{d}k_\perp G(k_\perp) e^{i\mathbf{k}_\perp \cdot \mathbf{b}}$$

QCD Cross section

$$\sigma_{QCD}(s) = \sum_{i,j,k,l} \int_{p_{T min}}^{s/4} \mathrm{d}p_T^2 \int_{4p_T^2/s}^{1} \mathrm{d}x_1 \int_{4p_T^2/x_1 s}^{1} \mathrm{d}x_2$$
$$\times \left[f_{i/A}(x_1, Q^2) f_{j/B}(x_2, Q^2) + f_{j/A}(x_1, Q^2) f_{i/B}(x_2, Q^2) \right]$$
$$\times \left[\frac{\mathrm{d}\hat{\sigma}_{ij\to kl}}{\mathrm{d}p_T^2}(\hat{t},\hat{u}) + \frac{\mathrm{d}\hat{\sigma}_{ij\to kl}}{\mathrm{d}p_T^2}(\hat{u},\hat{t}) \right] (1-\delta_{ij}/2)(1-\delta_{kl}/2)$$

$$\frac{\mathrm{d}\hat{\sigma}}{\mathrm{d}p_T^2} = \frac{\mathrm{d}\hat{\sigma}}{\mathrm{d}(-\hat{t})} \frac{\mathrm{d}(-\hat{t})}{\mathrm{d}p_T^2} = \frac{\mathrm{d}\hat{\sigma}}{\mathrm{d}(-\hat{t})} \frac{1}{\sqrt{1-4\frac{p_T^2}{\hat{s}}}} = \frac{\mathrm{d}\hat{\sigma}}{\mathrm{d}|\hat{t}|} \frac{1}{\sqrt{1-4\frac{p_T^2}{\hat{s}}}}$$

Analysis

Analysis

- We performed a χ^2 analysis at 90% C.L. using the CT18 PDF set at NLO, considering various cutoff choices for the DATA ensembles:

- $\sigma_{tot}^{pp,p\bar{p}}(10\,\mathrm{GeV} < \sqrt{s} < 1.8\,\mathrm{TeV};\ \mathbf{PDG}) + \rho^{pp,p\bar{p}}(10\,\mathrm{GeV} < \sqrt{s} < 1.8\,\mathrm{TeV};\ \mathbf{PDG}) +$
$\sigma_{tot}^{pp}(7, 8, 13\,\mathrm{TeV};\ \mathbf{ATLAS}) + \rho^{pp}(7, 8, 13\,\mathrm{TeV};\ \mathbf{ATLAS})$

- $\sigma_{tot}^{pp,p\bar{p}}(10\,\mathrm{GeV} < \sqrt{s} < 1.8\,\mathrm{TeV};\ \mathbf{PDG}) + \rho^{pp,p\bar{p}}(10\,\mathrm{GeV} < \sqrt{s} < 1.8\,\mathrm{TeV};\ \mathbf{PDG}) +$
$\sigma_{tot}^{pp}(2.76, 7, 8, 13\,\mathrm{TeV};\ \mathbf{TOTEM}) + \rho^{pp}(2.76, 7, 8, 13\,\mathrm{TeV};\ \mathbf{TOTEM})$

- $\sigma_{tot}^{pp,p\bar{p}}(10\,\mathrm{GeV} < \sqrt{s} < 1.8\,\mathrm{TeV};\ \mathbf{PDG}) + \rho^{pp,p\bar{p}}(10\,\mathrm{GeV} < \sqrt{s} < 1.8\,\mathrm{TeV};\ \mathbf{PDG}) +$
$\sigma_{tot}^{pp}(2.76, 7, 8, 13\,\mathrm{TeV};\ \mathbf{TOTEM}) + \rho^{pp}(2.76, 7, 8, 13\,\mathrm{TeV};\ \mathbf{TOTEM})$
$\sigma_{tot}^{pp}(7, 8, 13\,\mathrm{TeV};\ \mathbf{ATLAS}) + \rho^{pp}(7, 8, 13\,\mathrm{TeV};\ \mathbf{ATLAS})$

Fit Parameters

$$\sigma_{QCD}(s) = \mathcal{N} \sum_{i,j,k,l} \int_{p_{Tmin}}^{s/4} \mathrm{d}p_T^2 \int_{4p_T^2/s}^{1} \mathrm{d}x_1 \int_{4p_T^2/x_1 s}^{1} \mathrm{d}x_2$$
$$\times \left[f_{i/A}(x_1, Q^2) f_{j/B}(x_2, Q^2) + f_{j/A}(x_1, Q^2) f_{i/B}(x_2, Q^2) \right]$$
$$\times \left[\frac{\mathrm{d}\hat{\sigma}_{ij\to kl}}{\mathrm{d}p_T^2}(\hat{t}, \hat{u}) + \frac{\mathrm{d}\hat{\sigma}_{ij\to kl}}{\mathrm{d}p_T^2}(\hat{u}, \hat{t}) \right] (1 - \delta_{ij}/2)(1 - \delta_{kl}/2)$$

$$W_{SH}(b; \nu_{SH}) = \frac{\nu_{SH}^2}{96\pi} (\nu_{SH} b)^3 K_3(\nu_{SH} b)$$

Results

TOTEM

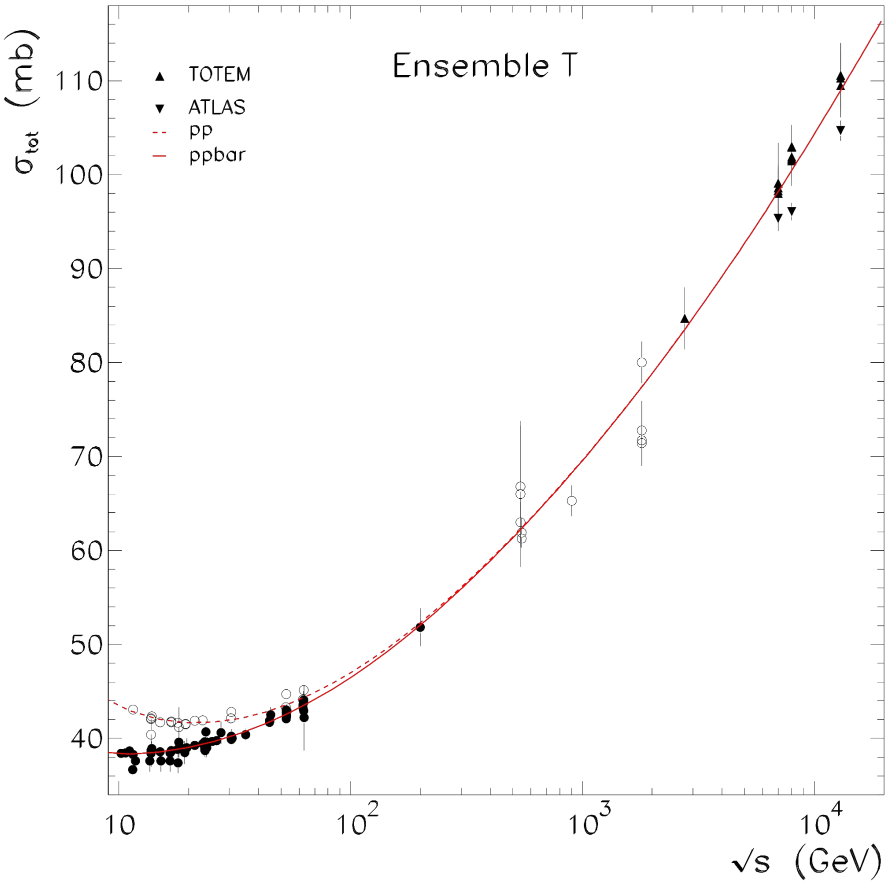

Ensemble T
TOTEM
ATLAS
pp
ppbar
σtot (mb)
110
100
90
80
70
60
50
40
10
10^2
10^3
10^4
√s (GeV)

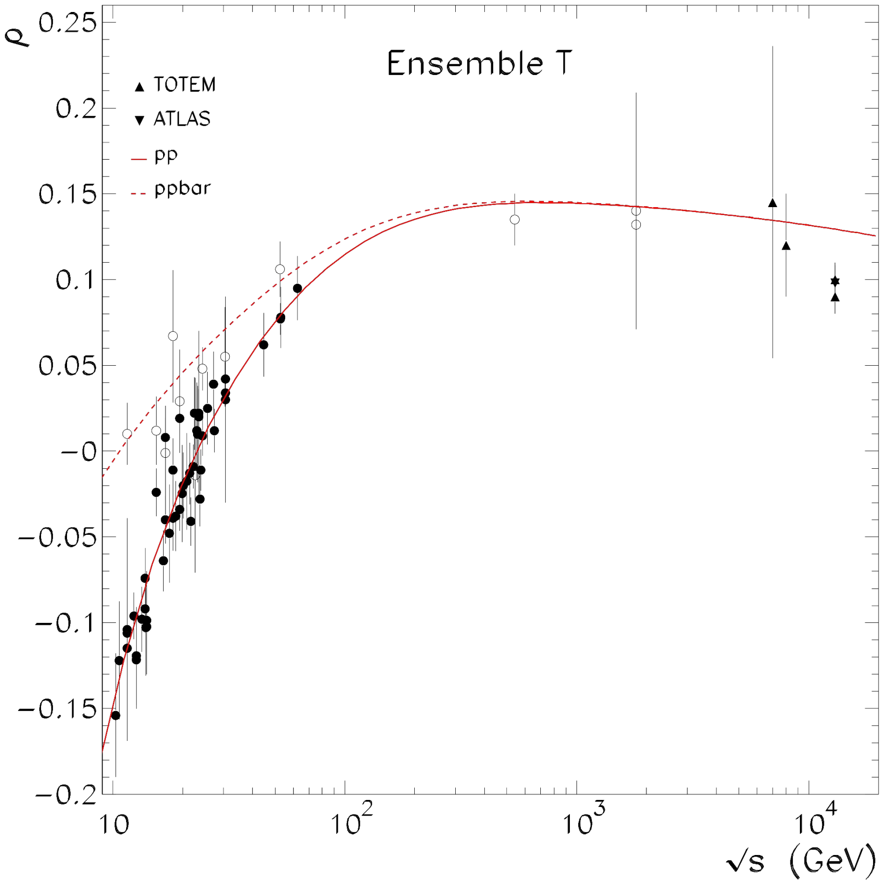

Ensemble T
TOTEM
ATLAS
pp
ppbar
ρ
0.25
0.2
0.15
0.1
0.05
−0
−0.05
−0.1
−0.15
−0.2
10
10^2
10^3
10^4
√s (GeV)

ALFA/ATLAS

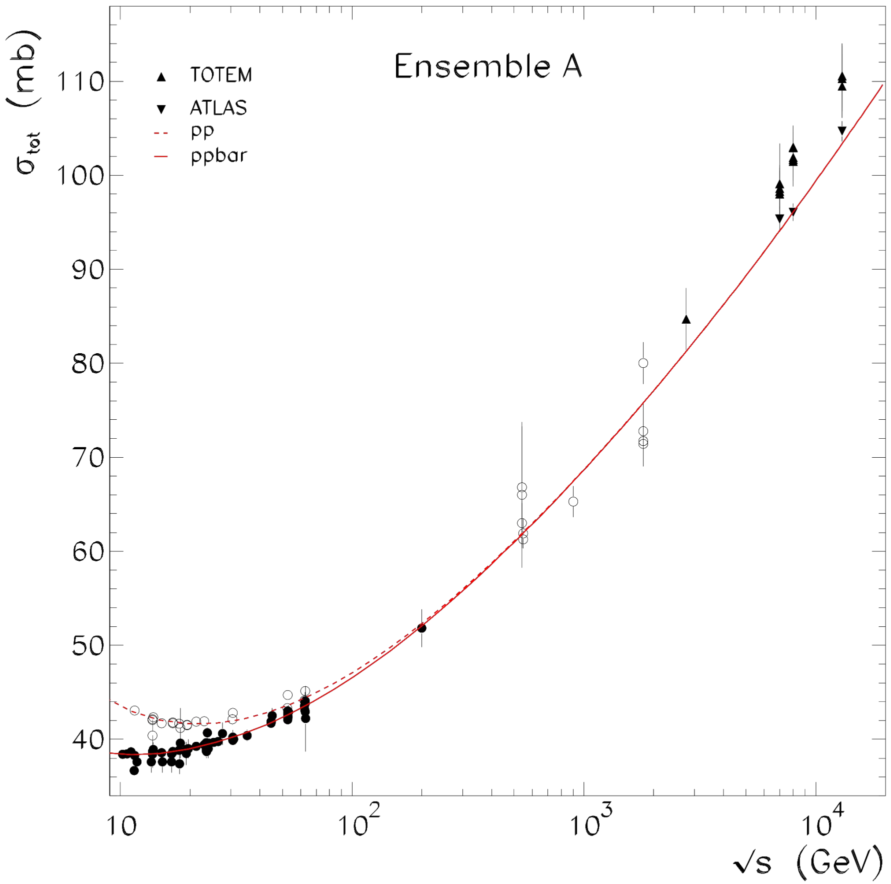

Ensemble A
TOTEM
ATLAS
pp
ppbar
σ_{tot} (mb)
$\sqrt{s}$ (GeV)

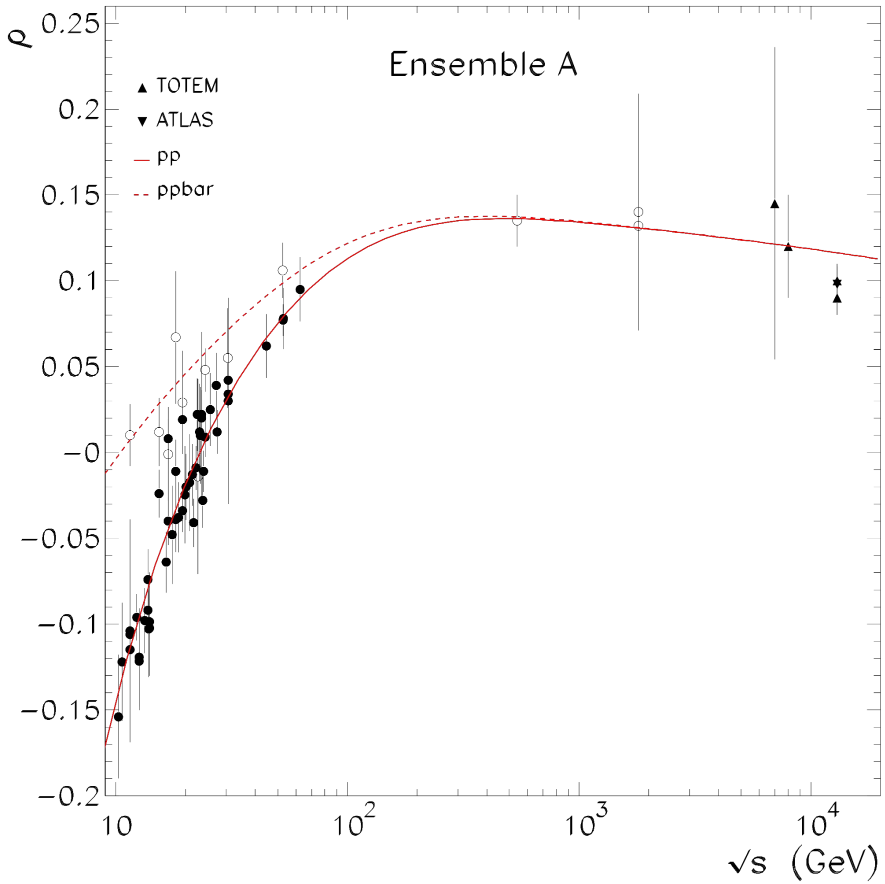

Ensemble A
TOTEM
ATLAS
pp
ppbar
ρ
$\sqrt{s}$ (GeV)

ALFA/ATLAS + TOTEM

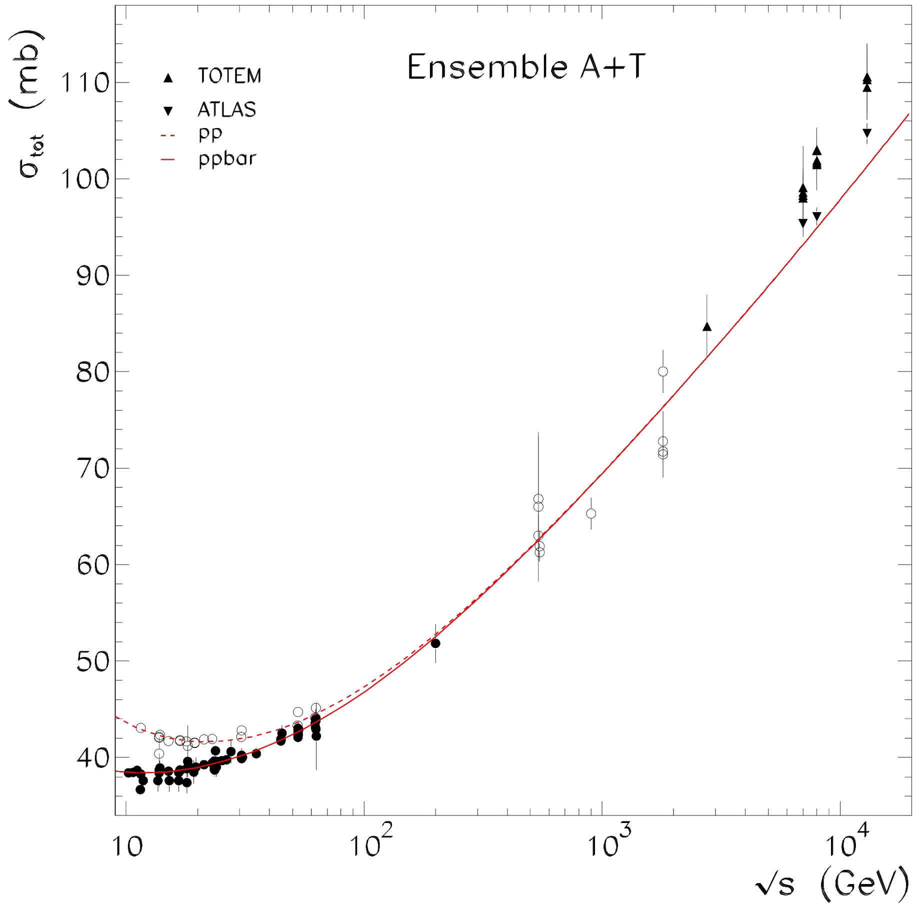

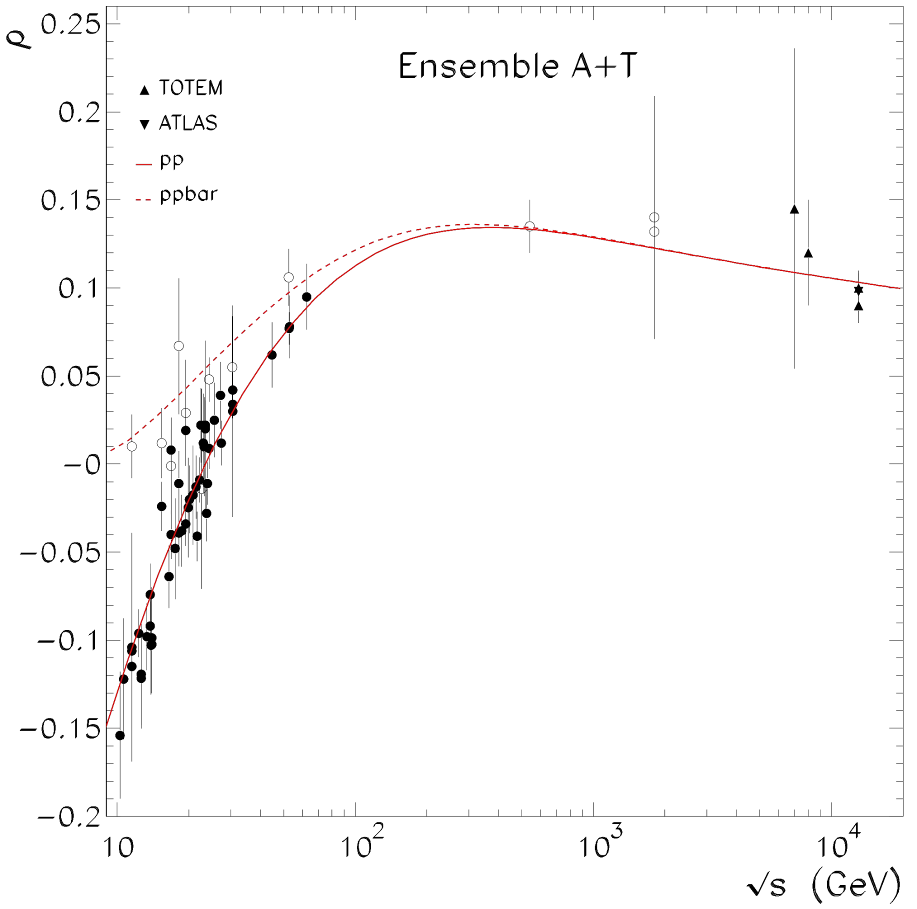

ANALYSIS RESULT

- The best cutoff for the choice of PDF, **CT18**, at next-to-leading order was found to be $p_{T_{min}} = 1.1$ GeV.

- Between **TOTEM** and **ALFA/ATLAS** data sets, the second present the global fit of the two.

- The choice of range for the **normalization factors** of the **ALFA/ATLAS** data points are based around their luminosity uncertainty for each energy.

- Regarding the **TOTEM** data points, the normalization factors were designed to ensure that the **lower bound of the average data values** at each energy level matches the minimum allowed limit for the **total cross section** of **ALFA/ATLAS** at the corresponding energies.

$p_{tmin} = 1.1$ GeV	TOTEM	ATLAS	TOTEM $\oplus$ ATLAS
$\mathcal{N}$	0.94 ± 0.03	1.14 ± 0.03	2.89 ± 0.11
ν_{SH} [GeV]	1.19 ± 0.04	1.36 ± 0.03	1.56 ± 0.02
$N_{0.9}[E]$	-	-	0.9570 [0.900 – 1.100]
$N_{1.8}[E]$	-	-	1.04870 [0.900 – 1.100]
$N_{1.8}[C]$	-	-	0.94130 [0.900 – 1.100]
$N_{2.76}[E]$	-	-	1.0400 [0.926 – 1.074]
$N_{7}[A]$	-	-	1.0230 [0.977 – 1.023]
$N_{8}[A]$	-	-	1.0120 [0.985 – 1.015]
$N_{13}[A]$	-	-	1.0215 [0.9785 – 1.0215]
$N_{7}[T]$	-	-	1.0540 [0.946 – 1.054]
$N_{8}[T]$	-	-	1.0740 [0.926 – 1.074]
$N_{13}[T]$	-	-	1.0700 [0.930 – 1.070]
ν	168	158	161
χ^2/ν	1.23	1.12	1.05

ATLAS Collaboration (G. Aad et al.), Nucl. Phys. B 889, 486 (2014).
ATLAS Collaboration (M. Aaboud et al.), Phys. Lett. B 761, 158 (2016)
ATLAS Collaboration (G. Aad et al.), Eur. Phys. J. C 83, 441 (2023)..

ANALYSIS RESULT

- This **adjustment** for **normalization factors improved** the global fit when compared to the fit with the data sets separated.

- When observing the results of the global fit for these normalization factors, it becomes evident why the generated curve for total cross section passes under the data points for both **ALFA/ATLAS** and **TOTEM**.

$p_{tmin} = 1.1\,\text{GeV}$	TOTEM	ATLAS	TOTEM $\oplus$ ATLAS
$\mathcal{N}$	0.94 ± 0.03	1.14 ± 0.03	2.89 ± 0.11
ν_{SH} [GeV]	1.19 ± 0.04	1.36 ± 0.03	1.56 ± 0.02
$N_{0.9}[E]$	-	-	0.9570 [0.900 – 1.100]
$N_{1.8}[E]$	-	-	1.04870 [0.900 – 1.100]
$N_{1.8}[C]$	-	-	0.94130 [0.900 – 1.100]
$N_{2.76}[E]$	-	-	1.0400 [0.926 – 1.074]
$N_{7}[A]$	-	-	1.0230 [0.977 – 1.023]
$N_{8}[A]$	-	-	1.0120 [0.985 – 1.015]
$N_{13}[A]$	-	-	1.0215 [0.9785 – 1.0215]
$N_{7}[T]$	-	-	1.0540 [0.946 – 1.054]
$N_{8}[T]$	-	-	1.0740 [0.926 – 1.074]
$N_{13}[T]$	-	-	1.0700 [0.930 – 1.070]
ν	168	158	161
χ^2/ν	1.23	1.12	1.05

ATLAS Collaboration (G. Aad et al.), Nucl. Phys. B 889, 486 (2014).
ATLAS Collaboration (M. Aaboud et al.), Phys. Lett. B 761, 158 (2016)
ATLAS Collaboration (G. Aad et al.), Eur. Phys. J. C 83, 441 (2023)..

Conclusion and Perspectives

Conclusions

- The chosen model adequately describes the high energy **LHC data** for both **ALFA/ATLAS** and **TOTEM** experiments.

- The procedure of allowing for a **normalization** of **high energy** data improved the global fit and permitted the **concurrently utilization** of **ALFA/ATLAS** and **TOTEM** data sets.

- This normalization procedure, although it doesn't describe the central value of $\boldsymbol{\rho}$ at $\sqrt{s}$ **= 13 TeV** for **ALFA/ATLAS,** it permits touching it's error bar.

Perspectives

- To utilize and study the effects of different sets of PDF’s with our current model, manly **MSHT20** and **NNPDF4.0.**
- To test the utilization of an **odd component** for the **semihard region** (**Odderon**).
- In future analysis we will look at different types of **form factors**, beyond **dipole**.
- Extend the utilization of the model to describe the differential cross section at $\sqrt{s}$ = **7 , 8** and **13 TeV**.

Thank You!!!